

**Research paper**

Assessment of the crushing strength of concrete rings reinforced with synthetic fibers

Agnieszka Głuszko¹, Lidia Buda-Ożóg²

Abstract: Since the 1990s, the technology of fiber-reinforced concrete has undergone significant development, initiated by the publication of the comprehensive ACI 544 committee report. Standardized methods for measuring the key mechanical properties of fiber-reinforced concrete are outlined in EN 14651 and ASTM C1609, while material properties are specified in CEN/TS 19101. It is widely known that the addition of fibers improves the properties of concrete; however, their effectiveness depends on various factors such as material type (metallic and non-metallic fibers), shape (crimped and fibrillated fibers), dimensions (length, diameter and slenderness), fiber volume in the concrete mix, and even the consistency of the mix. The aim of the experimental studies was to assess the load-bearing capacity of concrete produced under industrial conditions, modified with various synthetic fibers at different dosages. The primary selection criterion for the fibers was to meet the residual strength requirements of the tested element with the lowest possible weight fraction of dispersed reinforcement. In addition to determining the residual strength of PFRC, the study also measured compressive strength, flexural tensile strength, and the modulus of elasticity. The obtained results and force-crack width relationships were used to validate the numerical model of a standard notched beam. This calibrated material model was then used to develop a finite element model (FEM) and to conduct a preliminary assessment of the load-bearing capacity of prefabricated FRC rings using the ATENA software.

Keywords: fiber-reinforced concrete, FRC, polymer fibers, prefabricated rings, residual strength

¹MSc., Eng., Rzeszow University of Technology, Faculty of Civil Engineering, Al. Powstancow Warszawy 12, 35-959 Rzeszow, Poland, e-mail: agluszko@prz.edu.pl, ORCID: 0000-0002-9978-1323

²DSc., PhD., Eng., Rzeszow University of Technology, Faculty of Civil Engineering, Al. Powstancow Warszawy 12, 35-959 Rzeszow, Poland, e-mail: lida@prz.edu.pl, ORCID: 0000-0002-1205-1345

1. Introduction

Prefabricated concrete rings are vertical structural components of the manhole shaft characterized by a constant cross-sectional profile. They are widely used in road infrastructure, particularly in sewerage, water supply, and drainage systems. These rings constitute an integral part of prefabricated water-retaining structures (WRS), such as tanks, dams, pools, flood embankments, and other hydraulic installations designed for water storage, control, or management. Concrete used in sewer manhole rings is continuously exposed to groundwater, rainfall, harmful organic compounds, and salts present in wastewater, including sulfates, chlorides, nitrates, and ammonia. Typically, concrete rings are reinforced with single steel bars, wire coils, or – if the element has a small diameter and carries relatively low loads – remain unreinforced. Although traditional steel reinforcement provides high mechanical strength, it is susceptible to corrosion in aggressive environments characterized by high salt content, variable pH levels, and the presence of chemical and biological agents. Due to the porous and hydrophilic nature of concrete, chloride ions can penetrate to the surface of embedded steel, initiating corrosion processes. Corrosion not only reduces the load-bearing capacity of the reinforcement but also leads to deterioration of the concrete cover, thus accelerating the degradation of the entire structure and necessitating costly repairs [1, 2]. Consequently, increasing attention is being given to the use of corrosion-resistant reinforcement materials that simultaneously simplify and accelerate construction processes. The application of non-metallic dispersed reinforcement, such as fiber-reinforced concrete (FRC), represents an innovative solution that eliminates problems associated with steel corrosion and the need for conventional reinforcement assembly. In addition to enhanced durability, synthetic reinforcement offers advantages such as a lower carbon footprint, shorter construction times, and greater economic efficiency.

Since the 1990s, fiber-reinforced concrete technology has undergone significant advancements [3], initiated by the publication of the comprehensive ACI 544 committee report [1]. Testing methods for determining the mechanical properties of FRC have been standardized in EN 14651 [4] and ASTM C1609 [5], while material specifications are provided in CEN/TS 19101 [6], forming the basis for FRC design standards. It is widely acknowledged that the incorporation of fibers improves the overall performance of concrete [7]. Dispersed reinforcement is typically classified based on the modulus of elasticity of the fibers:

- Low-modulus fibers (e.g., nylon, polypropylene, polyethylene, polyester) primarily enhance crack resistance,
- High-modulus fibers (e.g., steel, carbon, glass) significantly improve both crack resistance and strength properties [8, 9].

Macrofibers provide substantial residual strength and post-cracking load transfer capabilities, enabling them to replace traditional steel reinforcement in structural applications. Microfibers, in contrast, mainly reduce plastic shrinkage and limit early-age cracking [10]. These properties contribute to enhanced durability, prolonged service life, and reduced maintenance costs. Polypropylene fibers, in particular, improve crack distribution control, thereby increasing the watertightness of concrete structures. Laboratory studies have demonstrated that even small additions of monofilament polypropylene fibers can significantly reduce water and chemical permeability, protecting concrete from frost damage and corrosion [11]. Due to

their excellent stability in aggressive environments, polypropylene fibers ensure the long-term durability of concrete components, which is critical for prefabricated rings exposed to harsh conditions. Adding a small volume fraction of randomly distributed polypropylene fibers enhances crack resistance, ductility, and impact resistance [12, 13]. Dispersed reinforcement increases the energy absorption capacity of concrete by several orders of magnitude compared to fiberless matrices, effectively mitigating brittle fracture phenomena [14, 15]. Furthermore, polypropylene fibers not only improve crack resistance and delamination resistance but also contribute to enhancements in tensile and flexural strengths [16, 17]. An optimal polypropylene fiber content of approximately 0.5% by volume has been reported for maximizing flexural strength, and 0.25% for compressive strength [18]. However, the effect of polypropylene fibers on compressive strength remains ambiguous, with studies reporting both increases [18] and decreases [19] relative to plain concrete. Other investigations [20, 21] have found no significant impact on compressive strength, although increases in tensile and flexural strengths have been observed with longer curing times and higher fiber contents [22, 23]. When evaluating the flexural strength of fiber-reinforced concrete, a significant increase in flexural strength was noted with increasing fiber content [24]. The elastic modulus of FRC is generally comparable to that of plain concrete [25], with slight increases over time [26]. The presence of fibers, however, significantly influences the workability of concrete mixes. Excessive fiber content leads to a marked deterioration of workability and, in extreme cases, can negatively affect mechanical properties due to increased porosity, permeability, and water absorption.

The primary objective of the experimental study was to optimize the dosage of polypropylene fibers under industrial conditions. The selection criterion was the fulfillment of standard residual strength requirements with the minimum necessary fiber content. In addition to residual strength, compressive strength, flexural tensile strength, and the elastic modulus of the polypropylene fiber-reinforced concrete (PFRC) were also determined. The obtained material properties were employed for the preliminary validation of the fiber-reinforced concrete through finite element modeling (FEM) of a notched beam specimen. The calibrated material model was subsequently used to develop the final FEM model and to conduct a preliminary load-bearing capacity assessment of prefabricated PFRC rings using the ATENA simulation software.

2. Materials




The concrete class C45/55 and the geometry of the concrete rings were adopted in accordance with the assumptions of the concrete manhole manufacturer. The detailed composition of the analysed concrete mixtures is presented in Table 1.

Three types of synthetic macrofibers – BC35, BC50, and MP40 – whose properties are listed in Table 2, were used in the tests. The letter code indicates the material from which the fibers were made, while the number specifies the fiber length. All fibers were monofilament and had tensile strengths ranging from 500 to 590 MPa, chemical resistance, densities between 0.91 and 0.92 g/cm³, and melting temperatures ranging of 160–170°C.

Table 1. Concrete strength class and components

	Cement (kg/m ³)	Fly ash (kg/m ³)	Sand/Gravel (kg/m ³)			Water (l)	w/c	Admixture Chryso (kg/m ³)		
			0/2	2/8	8/16			Premia	Air LB	Xel Time
CC1 – C45/55	380	100	690	480	490	131	0.345	4.3	3.0	3.84
CC2 – C45/55	350	100	750	480	490	160	0.457	2	0.2	6.4

Table 2. Fiber properties

	Contec 35 BC35	Contec 50 BC50	Nordica MP40
Base Material	bicomponent polyolefin	bicomponent polyolefin	modified polypropylene
Tensile Strength (MPa)	590	590	500
Elastic Modulus (GPa)	>11	>11	6
Diameter (mm)	0.5	0.5	0.7
Length (mm)	35	50	40
Aspect Ratio (l/d)	70	100	57
Form	macro monofilament	macro monofilament	macro monofilament
			

3. Experimental investigations

3.1. Research methods

The research encompassed two stages involving the preparation of concrete mixtures: one reference mixture without fibers and three mixtures incorporating fibers at dosages of 3.0 kg/m³, 3.5 kg/m³, and 4.0 kg/m³, as detailed in Table 3. In the first stage, aimed at comparing the strength of concrete based on the CC2 recipe with different types of fibers, concretes labeled PRFC3 to PRFC6 were prepared. Analysis of the results indicated that the PRFC4 mixture, containing MP40 fibers, exhibited the highest residual strength, leading to its selection for further investigation. The second stage involved comparing the strength parameters of concrete without fibers and with varying amounts of MP40 fibers. For this mixture (CC1), slight modifications were made to the aggregate grading curve and to the dosing of air-entraining and workability-improving admixtures, due to the variability of the raw materials used, as listed in Table 1.

Samples for testing were prepared and cured under industrial conditions at the manufacturer's prefabrication plant, reflecting the actual production environment of prefabricated manholes, in accordance with PN-EN 12390-1 [27] and PN-EN 12390-2 [28] standards.

Table 3. PFRC composite mixtures

	Concrete mixtures	Type of fiber	Dosage (kg/m ³)
CM1	CC1	–	–
PFRC1		MP40	3
PFRC2		MP40	3.5
PFRC3	CC2	MP40	3
PFRC4		MP40	4
PFRC5		BC35	3.5
PFRC6		BC50	4

According to PN-EN 12390-3 [29] and PN-EN 12390-4 [30], cube samples measuring $150 \times 150 \times 150$ mm and cylindrical samples measuring 150×300 mm were prepared from each mixture to determine compressive strength and elastic modulus. During the tests, the initial elastic modulus $E_{C,0}$, stabilized secant modulus $E_{C,S}$, and the average secant modulus E_{cm} were determined. The flexural tensile strength $f_{ct,m}$ was determined according to PN-EN 12390-5 [31], using a four-point bending configuration. The last destructive test involved determining the residual flexural strength of fiber-reinforced concrete (PFRC) using the three-point bending test (3PBT) in accordance with PN-EN 14651 [32]. Beams measuring $150 \times 150 \times 700$ mm were notched at mid-span to a depth of 25 mm and width of 5 mm. The destructive force was applied at mid-span, with displacement control at a rate of 0.05 mm/min up to a crack mouth opening displacement (CMOD) of 1 mm, and then 0.2 mm/min up to a CMOD of 4 mm. The F-CMOD (force–crack opening displacement) relationship was measured, and the residual flexural strength $f_{R,j}$ was determined according to PN-EN 14651 [32].

3.2. Compressive strength and elastic modulus

The compressive strength of concrete samples is presented in Table 4. The mean compressive strength f_{cm} , standard deviation s_{fc} , coefficient of variation V_{fc} , and characteristic strength were calculated. In the first stage of the study, the mean compressive strength f_{cm} ranged from 86.8 MPa to 89.9 MPa for PFRC3 to PFRC6. The coefficient of variation V_{fc} ranged from 0.9% to 2.1% for fiber-reinforced concretes containing MP40 fibers, and from 3.9% to 8.9% for concretes containing BC35 and BC50 fibers. The large variability in results could be due to difficulties encountered during mixing, related to the greater stiffness of BC35 and BC50 fibers compared to other fibers. The conducted tests did not show a significant influence of fiber type on the compressive strength of the tested samples. The authors of publication [33] indicated that when the fiber slenderness exceeded 75, the compressive strength and crack

resistance of concrete decreased. However, this observation was not confirmed in the conducted tests on cubic samples; only slight effects of fiber slenderness were observed in tests on cylindrical samples, as shown in Table 5. The second stage involved comparing the compressive strength of fiber-reinforced concrete with varying MP40 fiber contents to the reference concrete without dispersed reinforcement. The compressive strength f_{cm} of cubic samples increased by 2.4% and 4.4% for PFRC1 and PFRC2 concretes with fiber additions of 3.0 kg/m³ and 3.5 kg/m³, respectively, compared to the reference samples (CM1). For cylindrical samples, the compressive strength f_{cm} increased by up to 1%. Therefore, it can be concluded that the type and amount of fibers do not significantly affect f_{cm} , which is consistent with [24, 34]. The stabilized elastic modulus $E_{C,S}$ of concrete was determined according to Method A [35], and the results are shown in Table 6. The use of BC50 fibers, which have the highest elastic modulus (> 11 GPa) and the greatest slenderness, resulted in the highest elastic modulus value of the tested fiber-reinforced concrete PFRC6 – 53.5 GPa.

Table 4. Compressive strength of cubic specimens of PFRC

Dosage	$f_{c,cube}$ [MPa]												f_{cm} [MPa]	s_{fc} [MPa]	V_{fc} [%]	$f_{c,0.05}$ [MPa]
	1	2	3	4	5	6	7	8	9	10	11	12				
CM1	71.9	67.2	64.3	71.8	74.2	70.3	70.0	68.5	70.0	68.8	72.1	68.6	69.8	2.6	3.7	68.5
PFRC1	72.1	71.1	73.2	70.0	70.5	72.1	–	–	–	–	–	–	71.5	1.2	1.7	70.9
PFRC2	74.2	74.4	72.0	75.7	77.2	75.5	70.9	70.1	68.8	70.9	74.1	71.8	73.0	2.6	3.5	71.2
PFRC3	91.3	89.3	87.4	90.4	88.4	92.4	–	–	–	–	–	–	89.9	1.9	2.1	88.6
PFRC4	87.1	87.1	85.4	86.5	87.2	87.4	–	–	–	–	–	–	86.8	0.7	0.9	86.3
PFRC5	91.0	94.7	95.6	78.9	77.6	89.0	–	–	–	–	–	–	87.8	7.8	8.9	82.6
PFRC6	87.2	83.4	86.1	89.5	91.9	89.9	93.6	–	–	–	–	–	88.8	3.5	3.9	86.6

Table 5. Compressive strength of cylindrical specimens of PFRC

Dosage	$f_{c,cyl}$ [MPa]								f_{cm} [MPa]	s_{fc} [MPa]	V_{fc} [%]	$f_{c,0.05}$ [MPa]
	1	2	3	4	5	6	7	8				
CM1	54.0	59.4	61.4	61.0	56.6	61.2	58.6	59.6	59.0	2.6	4.3	57.5
PFRC1	45.9	65.3	64.9	65.9	–	–	–	–	60.5	9.7	16.1	49.1
PFRC2	58.7	62.7	57.7	60.5	59.8	59.2	63.5	63.9	60.8	2.3	3.8	59.4
PFRC3	82.4	83.6	80.3	86.9	–	–	–	–	83.3	2.8	3.3	80.1
PFRC4	86.0	85.2	84.5	86.4	–	–	–	–	85.5	0.8	1.0	84.5
PFRC5	46.2	77.4	82.8	80.1	–	–	–	–	71.6	17.1	23.9	51.5
PFRC6	78.1	76.3	72.5	77.2	–	–	–	–	76.0	2.5	3.2	73.1

Table 6. Elastic Modulus of PFRC

PFRC	$f_{c,cyl}$ [MPa]	σ_a [MPa]	$E_{C,S,1}$ [GPa]	$E_{C,S,2}$ [GPa]	$E_{C,S,3}$ [GPa]	E_{cm} [GPa]	s_{fc} [MPa]	V_{fc} [%]
CM1	54.0	18.0	37.0	35.5	35.3	35.9	1,1	3,0
PFRC1	45.9	15.3	36.0	36.4	34.8	35.7	0.8	2.3
PFRC3	82.4	27.5	44.7	51.1	46.7	47.5	3.3	6.9
PFRC4	86.0	28.7	46.5	44.2	43.7	44.8	1.5	3.3
PFRC5	46.2	15.4	45.0	50.9	48.2	48.0	3.0	6.2
PFRC6	78.1	26.0	51.2	55.8	90.8	53.5	3.3	6.1

3.3. Flexural tensile strength and residual strength

The tensile strength of concrete in flexure obtained from the tests is summarized in Table 7. A slight decrease in the flexural tensile strength of fiber-reinforced concrete elements was observed compared to the strength determined for the reference concrete samples (CM1) which is not consistent with the results of many studies presented in the literature. However, it should be noted that the tested concrete was produced under industrial conditions, where the water-cement ratio could vary slightly due to the moisture content of the aggregate or the preparation of the concrete mix. The test results showed that the reference concrete (without fibers) had the highest average flexural strength, but also the greatest heterogeneity of the results obtained, with the highest coefficient of variation exceeding 12.5%.

Table 7. Flexural tensile strength of PFRC beam specimens

	f_{ct} [MPa]						$f_{ct,m}$ [MPa]	s_{fct} [MPa]	V_{fct} [%]
	1	2	3	4	5	6			
CM1	6.82	7.84	6.86	5.39	6.45	6.09	6.6	0.8	12.5
PFRC1	6.12	5.74	5.64	–	–	–	5.8	0.3	4.3
PFRC2	5.85	7.21	6.00	5.16	6.32	5.81	6.1	0.7	11.2
PFRC3	4.64	4.85	4.96	–	–	–	4.8	0.2	3.4
PFRC4	5.12	5.62	4.98	–	–	–	5.2	0.3	6.4
PFRC5	5.50	5.16	5.37	–	–	–	5.3	0.2	3.2
PFRC6	5.47	5.67	4.93	–	–	–	5.4	0.4	7.1

The subsequent stage of the research focused on determining the residual flexural tensile strength within the limit of proportionality (LOP, $f_{ct,L}^f$) with three specimens tested for each type of concrete. The recorded F –CMOD curves were transformed, in accordance with [32], into $f_{R,j}$ –CMOD curves, with averaged values presented in Fig. 1(a). A distinct peak in the

force $f_{R,j}$ was observed in the initial loading phase, indicating a high load transfer capacity immediately following crack initiation. The load–deflection curves of the PFRC1, PFRC2, PFRC4, and PFRC6 concrete mixtures exhibited pronounced post-cracking hardening behavior, indicating that MP40 and BC50 fibers possess superior crack-bridging capabilities. Notably, the F –CMOD relationships for individual samples within each series exhibited considerable variability, likely attributable to the limited crack surface area and the high statistical variation in the number of fibers effectively engaged in stress transfer across the notch. It was also observed that FRC specimens containing fibers with higher stiffness exhibited greater variability in the test results, confirming the increased tendency of stiff fibers to distribute unevenly within the concrete mix. In all samples, as similarly reported in [36], quasi-vertical cracks initiating within the notch area were observed, which did not lead to complete failure of the specimens. Figure 1(b) presents the mean force values accompanied by error bars, indicating the dispersion of results for crack mouth opening displacements (CMOD) ranging from 0.5 mm to 3.5 mm. Figure 2 shows a graphical comparison of the residual strengths f_{R1} , f_{R2} , f_{R3} and f_{R4} obtained from the tested samples. Based on the results, PFRC4 concrete with a fiber content of 4 kg/m³ was selected for further analysis, as it was the only mix that satisfied the minimum residual strength requirements: $f_{R,1}$ is equal 1.5 MPa at 0.5 mm CMOD and $f_{R,4}$ is equal 1.0 MPa at 3.5 mm CMOD, in accordance with PN-EN 14889-1:2007 [37].

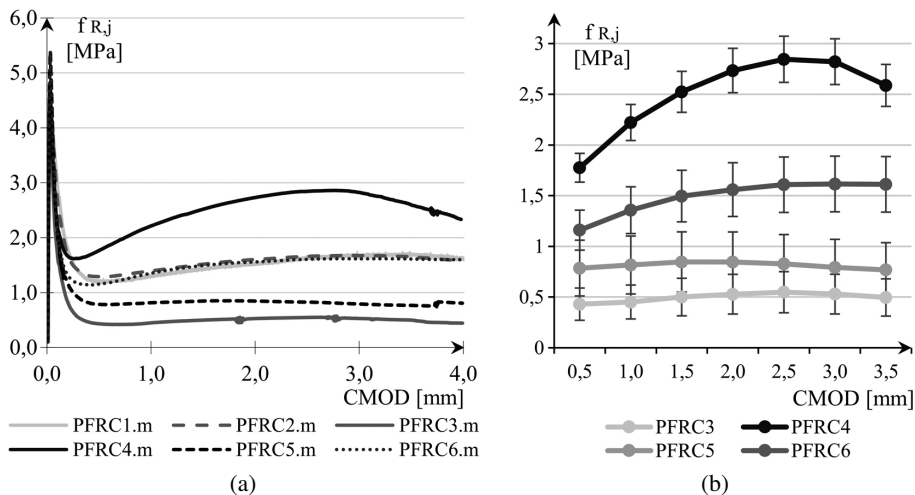


Fig. 1. $f_{R,j}$ –CMOD curves for PFRC: (a) mean values, (b) mean values with average coefficient of variation

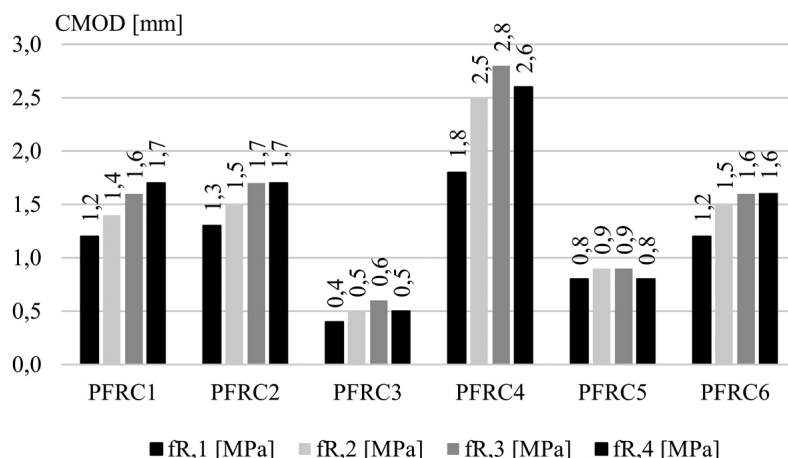


Fig. 2. Residual flexural tensile strength corresponding to CMOD (mean value)

4. Numerical analysis

4.1. FRC material model

The results of the experimental tests were used as input data for a numerical inverse analysis aimed at determining optimal bilinear force–crack mouth opening displacement (F – $CMOD$) relationships. The inverse analysis procedure developed by Olesen [38] was employed to identify the parameters of the fiber-reinforced concrete (FRC) material model based on experimental results from three-point bending tests (3PBT). This method involves fitting theoretical force–displacement curves to the experimental bending test data in order to derive the stress–crack opening relationship.

The beam was modeled using GID and ATENA 2024 software (Červenka Consulting) as a rectangular, symmetric 2D structure with a centrally located notch to facilitate controlled crack initiation, as shown in Fig. 3. A regular, structured mesh with an element size of 5 mm was applied. Given the notch dimensions at mid-span (25 mm in depth and 5 mm in width), mesh element sizes of 2.5 mm and 5 mm were evaluated in the numerical model. Since the results obtained using the 2.5 mm and 5 mm FE meshes differed only slightly, and the 5 mm mesh resulted in a significantly shorter simulation time, the 5 mm mesh was selected. Isoparametric quadrilateral plane elements with bilinear interpolation and four Gauss integration points were employed. Along the vertical axes of the notch edges, monitoring points were implemented to track crack development. *Constraint Points* were defined at the beam supports to establish boundary conditions and displacement constraints. Concrete was modeled as a nonlinear material utilizing the *CC3DNonLinCementitious2User* material model, which is specifically designed for simulating the behavior of fiber-reinforced concrete. This model incorporates the added fracture energy approach proposed by Juhász [39], which modifies the tension-softening branch of the stress–crack width curve to enhance the material’s ductility. The approach

accounts for the additional energy contributed by fibers during the cracking process, reflecting mechanisms such as fiber debonding, bridging, and pull-out, thus allowing a more accurate representation of FRC behavior under load. Steel supports were modeled as linearly elastic materials (*SOLID Elastic*), simulating a non-deformable contact. Loading was applied via a vertical displacement of 1 mm at the center of the upper steel plate, progressing in two stages up to a total displacement of 7 mm. In the first stage, the load was applied over 20 steps with an interval multiplier of 0.1; in the second stage, it was applied over 100 steps with an interval multiplier of 5.

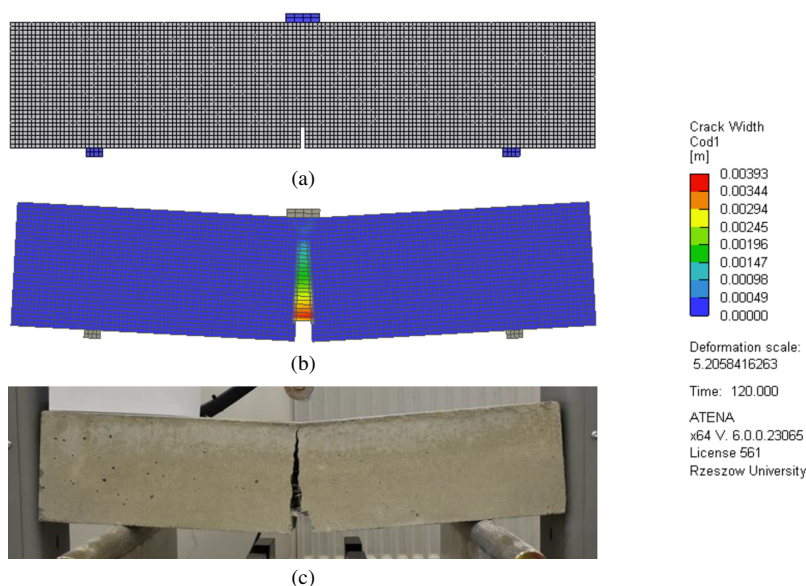


Fig. 3. Sample (a) before and (b) after numerical FEM and (c) after experimental residual tensile strength test

An iterative procedure was conducted, in which an initial bilinear numerical model (commonly referred to as the softening function) was assumed, and preliminary material parameters based on mean values were adopted, including ($f_{c,cube}$, $f_{c,cyl}$, E_{cm} , $f_{ct,m}$). Subsequently, the model response was obtained in the form of a force–displacement curve (e.g. ATENAexp1) and compared against the experimental results (PFRC4.m), as shown in Fig. 4.

Special attention was paid to the tensile function, as it determines the shape of the load–displacement diagram and the position of its peak. In the case of significant discrepancies between the numerical and experimental curves, the relative stresses in the tensile function were adjusted proportionally to the difference between the calculated and the expected bending force. This process started on ATENAexp1 curve and was repeated until satisfactory agreement was achieved. This method has been successfully applied in previous studies [40,41], where the behavior of FRC reinforced with steel fibers was simulated using inverse analysis based on the cohesive crack model. The model incorporating the identified parameters demonstrated very good agreement with the experimental data in terms of the F –CMOD curves, as presented

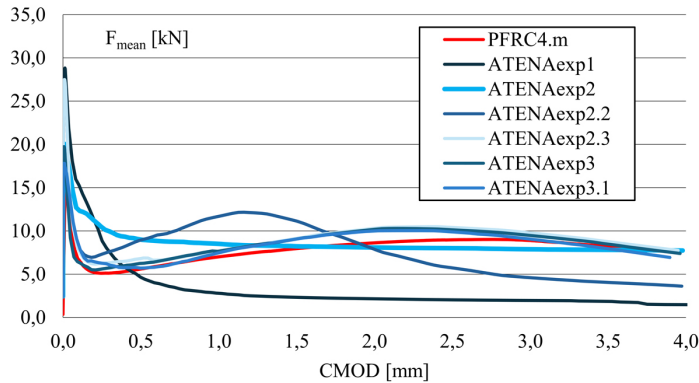


Fig. 4. F_{mean} –CMOD curves for PFRC4 from experimental and numerical inverse analysis

in Fig. 5. The behavior of the model indicated an accurate representation of FRC material performance, particularly accounting for energy absorption by the fibers following crack initiation. The calibrated material model was subsequently used to develop the final finite element model (FEM) and to perform a preliminary assessment of the load-bearing capacity of fiber-reinforced precast concrete rings using the ATENA software.

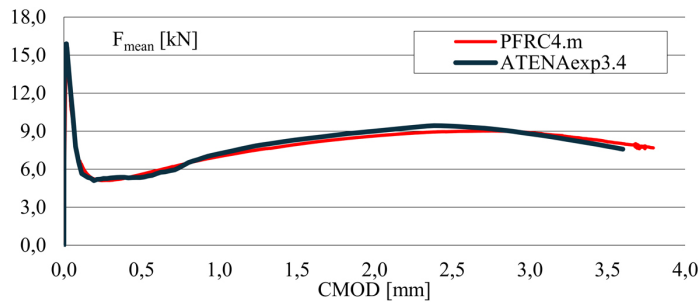


Fig. 5. Comparison material model from experimental data with final material model obtained from numerical inverse analysis

Based on the F –CMOD model fitted to the experimental data presented in Figure 5, taking into account the standard deviation of the test results and the number of samples tested, the F –CMOD dependence for characteristic values was determined.

4.2. Assessment of the crushing strength of fiber-reinforced concrete rings in accordance with PN-EN 1917

To evaluate the effectiveness of dispersed fiber reinforcement as an alternative to conventional metallic reinforcement, numerical simulations were performed replicating typical load-bearing and deformability tests for concrete rings. The FEM model for the concrete ring crushing test was developed in accordance with the standards PN-EN 1917 [42] and PN-EN

476 [43]. The precast concrete element was modeled as a 3D solid body with an internal diameter of 1500 mm, a wall thickness of 150 mm, and a height of 500 mm. The cross-section of the tested element is shown in Fig. 6(a), while the loading setup and finite element mesh division are illustrated in Fig. 6(b). In the numerical analysis, isoparametric quadrilateral plane elements with bilinear displacement interpolation (4-node elements) were employed. The load was applied vertically along the y -axis in two stages. In the first stage, a displacement of 0.2 mm was applied over 100 steps with an interval multiplier of 6, in the second stage, a displacement of 1 mm was applied over 100 steps with an interval multiplier of 50. The concrete ring was modeled using the previously calibrated *CC3DNonLinCementitious2User* material model, while the steel supports were defined as linearly elastic materials (*SOLID Elastic*). A *Master–Slave* contact formulation was applied between the surfaces of the concrete and steel elements, ensuring displacement compatibility between the non-conforming meshes of both materials. In this approach, the steel surface was defined as the *Slave* and the concrete surface as the *Master*. To ensure model stability and accurately simulate the real structural behavior, boundary conditions were imposed: displacements were fully restrained (in the x , y , and z directions) at the bottom support, and restrained in the x and z directions at the top support. During the analysis, vertical y and horizontal x displacements were monitored. The maximum deformation of the structure is presented in Fig. 7, while the force-displacement relationship obtained from the numerical analysis is shown in Fig. 8.

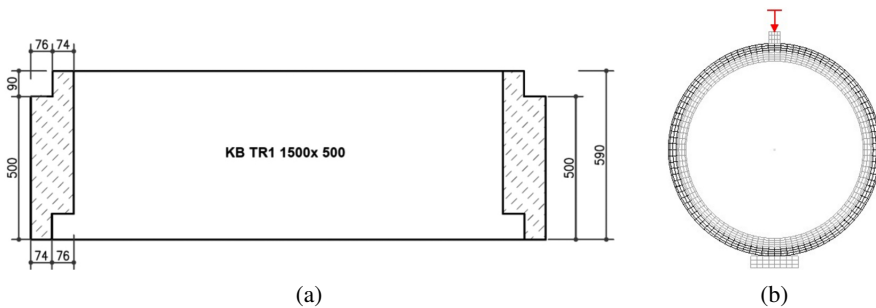


Fig. 6. Prefabricated fiber reinforcement PFRC4 ring: (a) geometric parameters, (b) axial load

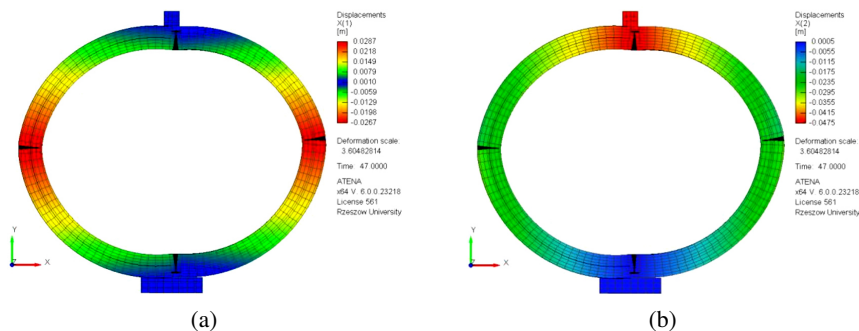


Fig. 7. Maximum displacement: (a) x -direction, (b) y -direction

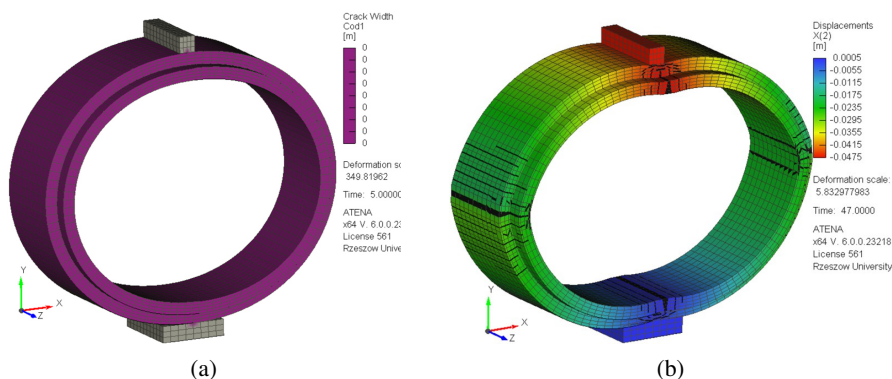


Fig. 8. Numerical model of the ring: (a) Crack width for F_c , (b) Collapse model of the ring

Requirements for a steel fiber-reinforced working chamber element or manhole shaft element (ring) as a concrete product, according to PN-EN 1917, state that it shall withstand a specified test load of $F_c = 0.67F_n$ without showing any signs of distress, where F_n is the minimum crushing load. In accordance with the PN-EN 476 [43] standard, the minimum crushing strength F_n of a concrete ring should be 25 kN per meter of length and crushing strength F_u of a concrete ring should be higher than F_n . Thus, for the analyzed ring with a length of 0.5 m, the required minimum strength is 12.5 kN. The conducted investigations demonstrated that the shaft wall element achieved a mean crushing strength exceeding $F_u = 41.2$ kN, significantly surpassing the normative requirements. Additionally, according to the standard, the shaft wall or working chamber element should withstand a crack initiation load F_c equal to $0.67F_n$ without the occurrence of continuous surface cracks wider than 0.3 mm over an uninterrupted length of 300 mm in the tension zones of the concrete. For a test load of $F_c = 8.4$ kN, no surface cracking of the shaft wall concrete was observed until $F = 28.3$ kN, as shown in Fig. 8(a). The final condition of the ring after failure, including x -direction displacement and cross-sectional cracking, is presented in Fig. 8(b).

4.3. Assessment of the serviceability of fiber-reinforced concrete rings accordance the FIB Model Code

According to the FIB Model Code 2010 [44], in all FRC structural elements that do not contain the minimum amount of conventional reinforcement, at least one of the following conditions must be satisfied:

$$(4.1) \quad \delta_u \geq 20\delta_{SLS}$$

$$(4.2) \quad \delta_{peak} \geq 5\delta_{SLS}$$

where: δ_u – ultimate displacement, δ_{peak} – displacement at the maximum load, δ_{SLS} – the displacement at service load computed by performing a linear elastic analysis with the assumptions of uncracked condition and initial elastic Young's modulus.

In order to assess the suitability of the analysed elements in accordance with relations (4.1) and (4.2), numerical simulations of the crushing of a fiber-reinforced concrete ring were performed, similarly to point 4.2. The numerical simulations took into account the characteristic values of the material parameters of fiber-reinforced concrete – PFRC4.

The numerical simulations took into account the characteristic values of the material parameters of fiber-reinforced concrete – PFRC4. The characteristic values were determined in accordance with Annex D of PN-EN 1990 – ‘Design with the use of test data’, section D7.2 – ‘Estimated characteristic values’, taking into account the sample size – 3 elements, and the coefficient of variation of individual test results presented in Tables 4 to 7.

The initial portion of the force-displacement relationship was found to be linear up to the occurrence of the first crack in the fiber-reinforced concrete (FRC) element, corresponding to a characteristic load of $F = 26.08$ kN and a service load displacement of $\delta_{SLS} = 0.38$ mm. The maximum characteristic load sustained by the shaft wall was $F = 39.5$ kN, corresponding to a measured vertical displacement of $\delta_{peak} = 1.28$ mm. Upon exceeding the tensile strength of concrete, a decrease in characteristic load capacity was observed down to $F = 20.9$ kN, followed by a strengthening phase reaching $F = 31.6$ kN, accompanied by increasing displacements up to failure at $\delta_u = 48$ mm, as shown in Fig. 9.

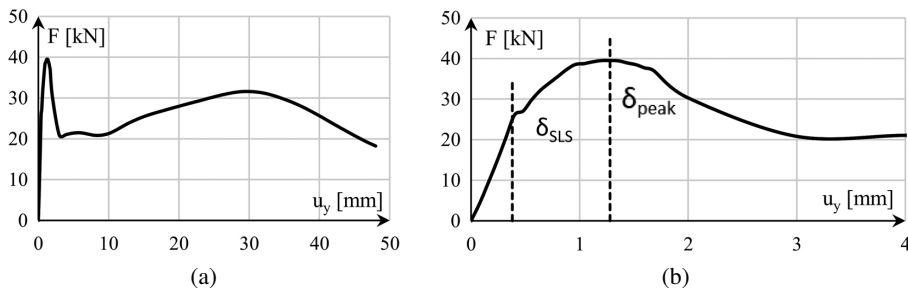


Fig. 9. Result from crushing strength numerical test of working chamber element (ring): (a) characteristic value of the force-displacement diagram until damage, (b) characteristic value of the force-displacement diagram until 4 mm

In the analysed case, only the condition expressed by Equation (4.1) was satisfied. However, the material behavior under loading, represented by the force-displacement relationship (Fig. 8), did not exhibit a sudden brittle failure typically associated with plain concrete, but rather showed a distinct plastic plateau. The ability of the model to sustain further loading after exceeding the tensile strength and the initiation of cracking confirms the effectiveness of fiber incorporation in enhancing the ductility and post-cracking load-bearing capacity of concrete.

5. Conclusions

Based on the experimental investigations and numerical analyses, the following general and specific conclusions were drawn

General conclusions:

- The use of synthetic macrofibers in precast concrete enables compliance with normative requirements for residual strength, confirming their suitability as an alternative to conventional steel reinforcement in aggressive environments.
- As shown by numerical simulations of the elimination of conventional steel reinforcement in favour of synthetic distributed reinforcement, a multi-criteria assessment of the analysed prefabricated elements is required, taking into account their crushing strength, deformability and, ultimately, the loads resulting from their installation.

Specific conclusions:

- The MP40 fibers dosed at 4 kg/m^3 (PFRC4) met the required residual strength criterion with the minimum necessary dosage according to PN-EN 14889-1:2007 [37]. According to fib Model Code 2010, this corresponds to class “1.5e” which indicates a post-cracking residual tensile strength of 1.8 MPa at CMOD = 0.5 mm and 2.8 MPa at CMOD = 2.5 mm. This class reflects pseudo-hardening behavior and may allow partial or full substitution of traditional reinforcement depending on structural requirements.
- No significant effect of synthetic fiber addition on compressive strength was observed, while an increase in the elastic modulus of concrete was noted with increasing fiber slenderness.
- Flexural tensile strength was strongly dependent on both the type and dosage of fibers, with the highest values recorded for PFRC5 and PFRC6, which incorporated fibers with a high elastic modulus.
- The introduction of dispersed reinforcement significantly improved crack resistance and crack propagation behavior, with macro-crack bridging mechanisms and enhanced post-cracking energy absorption capacity being observed.
- The material model calibrated based on notched beam tests showed very good agreement with the experimental results, enabling its use in finite element modeling (FEM) to assess the load-bearing capacity of actual precast elements.
- The numerical analysis of the ring, in relation to the requirements specified in PN-EN 476 [43], demonstrated compliance with a considerable safety margin.
- Throughout the conducted numerical simulations, no sudden brittle failure of the tested rings was observed. The application of an adequate amount of polymeric reinforcement allowed the shift of the failure mechanism from a dangerous brittle mode – typical of plain concrete elements – to a ductile behavior characterized by a distinct plastic plateau and the capacity for substantial deformations after the initiation of first cracks.

Acknowledgements

“The Regional Centre of Excellence in Engineering for Quality of Life and Technological Development”, funded by a subsidy from the Minister of Science and Higher Education under “The Regional Initiative of Excellence” Program (Project No. RID/SP/0032/2024/01)

References

- [1] ACI Committee 222, Corrosion of Metals in Concrete, *ACI Manual of Concrete Practice, Part-1*. ACI, 1992.

- [2] S. Jain and B. Pradhan, "Fresh, mechanical, and corrosion performance of self-compacting concrete in the presence of chloride ions", *Construction and Building Materials*, vol. 247, art. no. 118517, 2020, doi: [10.1016/j.conbuildmat.2020.118517](https://doi.org/10.1016/j.conbuildmat.2020.118517).
- [3] M.G. Alberti, "Polyolefin Fiber-Reinforced Concrete: From Material Behaviour to Numerical and Design Considerations", Ph.D. dissertation, Universidad Politécnica de Madrid, Spain, 2015.
- [4] EN 14651:2005+A1:2007 Test Method for Metallic Fiber Concrete – Measuring the Flexural Tensile Strength. European Committee for Standardization, Brussels.
- [5] ASTM C1609/C1609M-19 Standard Test Method for Flexural Performance of Fiber-Reinforced Concrete (Using Beam with Third-Point Loading). ASTM International, West Conshohocken, PA, 2019.
- [6] CEN/TS 19101:2005 Design of Fiber Concrete Structures. European Committee for Standardization, Brussels.
- [7] A.M. Brandt, "Fiber reinforced cement-based (FRC) composites after over 40 years of development in building and civil engineering", *Composite Structures*, vol. 86, pp. 3–9, 2008.
- [8] S.U. Islam and S.A. Waseem, "An experimental study on mechanical and fracture characteristics of hybrid fiber reinforced concrete", *Structures*, vol. 68, art. no. 107053, 2024, no. doi: [10.1016/j.istruc.2024.107053](https://doi.org/10.1016/j.istruc.2024.107053).
- [9] I.M.G. Bertelsen, L.M. Ottosen, and G. Fischer, "Quantitative analysis of the influence of synthetic fibers on plastic shrinkage cracking using digital image correlation", *Construction and Building Materials*, vol. 199, pp. 124–137, 2019, doi: [10.1016/j.conbuildmat.2018.11.268](https://doi.org/10.1016/j.conbuildmat.2018.11.268).
- [10] I. Markovic, "High-Performance Hybrid-Fiber Concrete", PhD thesis, Delft University, Netherland, 2006.
- [11] A. Richardson, "Polypropylene fibers in concrete with regard to durability," *Structural Survey*, vol. 21, no. 2, pp. 87–94, 2003.
- [12] A. El-Newihy, P. Azarsa, R. Gupta, and A. Biparva, "Effect of polypropylene fibers on self-healing and dynamic modulus of elasticity recovery of fiber reinforced concrete", *Fibers*, vol. 6, no. 1, 2018, doi: [10.3390/fib6010009](https://doi.org/10.3390/fib6010009).
- [13] I.A. Memon, A.A. Jhatial, S. Sohu, M.T. Lakhari, and Z.H. Khaskheli, "Influence of fiber length on the behaviour of polypropylene fiber reinforced cement concrete", *Civil Engineering Journal*, vol. 4, no. 9, pp. 2124–2131, 2018, doi: [10.28991/cej-03091144](https://doi.org/10.28991/cej-03091144).
- [14] Y. Wang, S. Backer, and V.C. Li, "An experimental study of synthetic fiber reinforced cementitious composites", *Journal of Materials Science*, vol. 22, no. 12, pp. 4281–4291, 1987.
- [15] B. Cotterell and Y.W. Mai, *Fracture Mechanics of Cementitious Materials*. Boca Raton, FL, USA: CRC Press, 1995, doi: [10.1201/9781482269338](https://doi.org/10.1201/9781482269338).
- [16] R. Khan and K.A. Rahman, "Mechanical properties of polypropylene fiber reinforced concrete for M25 & M30 mixes: A comparative study", *International Journal of Scientific Engineering and Applied Science (IJSSEAS)*, vol. 1, no. 5, pp. 327–340, 2015.
- [17] V. Afroughsabet and T. Ozbakkaloglu, "Mechanical and durability properties of high-strength concrete containing steel and polypropylene fibers", *Construction and Building Materials*, vol. 94, pp. 73–82, 2015, doi: [10.1016/j.conbuildmat.2015.06.051](https://doi.org/10.1016/j.conbuildmat.2015.06.051).
- [18] A.N. Ede and A.O. Ige, "Optimal polypropylene fiber content for improved compressive and flexural strength of concrete", *IOSR Journal of Mechanical and Civil Engineering*, vol. 11, no. 1, pp. 129–135, 2014.
- [19] A.E. Richardson and S. Landless, "Compressive strength of concrete with polypropylene fiber additions", *Structural Survey*, vol. 24, no. 2, pp. 138–153, 2006.
- [20] no. C.S. Das, T. Dey, R. Dandapat, B.B. Mukharjee, and J. Kumar, "Performance evaluation of polypropylene fiber reinforced recycled aggregate concrete", *Construction and Building Materials*, vol. 189, pp. 649–659, 2018, doi: [10.1016/j.conbuildmat.2018.09.036](https://doi.org/10.1016/j.conbuildmat.2018.09.036).
- [21] J. Błazy, Ł. Drobiec, and P. Wołka, "Mechanical properties of polymer fibre reinforced concrete in the light of various standards", *Archives of Civil Engineering*, vol. 70, no. 2, pp. 323–342, 2024, doi: [10.24425/ace.2024.149866](https://doi.org/10.24425/ace.2024.149866).
- [22] M. Nili and V. Afroughsabet, "The effects of silica fume and polypropylene fibers on the impact resistance and mechanical properties of concrete", *Construction and Building Materials*, vol. 24, no. 6, pp. 927–933, 2010, doi: [10.1016/j.conbuildmat.2009.11.025](https://doi.org/10.1016/j.conbuildmat.2009.11.025).
- [23] M. Małek, W. Łasica, M. Kadela, J. Kluczyński, and D. Dudek, "Physical and mechanical properties of polypropylene fiber-reinforced cement–glass composite", *Materials*, vol. 14, no. 3, 2021, doi: [10.3390/ma14030637](https://doi.org/10.3390/ma14030637).

- [24] Z.-h. Zhu, Y. Xiao, H.-j. Zhu, S.-no.d. Hu, and C. Yue, "Preparation and mechanical properties of polypropylene fiber reinforced calcined kaolin-fly ash based geopolymer", *Construction and Building Materials*, vol. 4, pp. 1139–1143, 2010.
- [25] Ł. Drobiec and J. Blazy, "Współczesne niemetaliczne zbrojenie rozproszone stosowane w konstrukcjach betonowych", *Izolacje*, vol. 61, no. 5, pp. 70–84, 2020.
- [26] P. Smarzewski, "Effect of curing period on properties of steel and polypropylene fiber reinforced ultra-high performance concrete", *IOP Conference Series: Materials Science and Engineering*, vol. 245, art. no. 032059, 2017, doi: [10.1088/1757-899X/245/3/032059](https://doi.org/10.1088/1757-899X/245/3/032059).
- [27] PN-EN 12390-1:2012 Testing hardened concrete – Part 1: Shape, dimensions and other requirements for specimens and moulds. Polish Committee for Standardization, Warsaw, 2012.
- [28] PN-EN 12390-2:2012 Testing hardened concrete – Part 2: Making and curing specimens for strength tests. Polish Committee for Standardization, Warsaw, 2012.
- [29] PN-EN 12390-3:2019 Testing hardened concrete – Part 3: Compressive strength of test specimens. Polish Committee for Standardization, Warsaw, 2019.
- [30] PN-EN 12390-4:2019 Testing hardened concrete – Part 4: Compressive strength – Specification for testing machines. Polish Committee for Standardization, Warsaw, 2019.
- [31] PN-EN 12390-5:2019-08 Testing hardened concrete – Part 5: Flexural strength of test specimens. Polish Committee for Standardization, Warsaw, 2019.
- [32] PN-EN 14651:2007 Test method for metallic fiber concrete – Measuring the flexural tensile strength (limit of proportionality (LOP), residual). Polish Committee for Standardization, Warsaw, 2007.
- [33] M.S. Shetty and A.K. Jain, *Concrete Technology: Theory and Practice*. New Delhi: S Chand and Company Ltd., 2010.
- [34] M. Hsie, C. Tu, and P.S. Song, "Mechanical properties of polypropylene hybrid fiber-reinforced concrete", *Materials Science and Engineering A*, vol. 494, no. 1–2, pp. 153–157, 2008.
- [35] PN-EN 12390-13:2014-02 Testing hardened concrete – Part 13: Determination of secant modulus of elasticity in compression. Polish Committee for Standardization, Warsaw, 2014.
- [36] J. Blazy, Ł. Drobiec, and P. Wolka, "Flexural tensile strength of concrete with synthetic fibers", *Materials*, vol. 14, no. 16, 2021, doi: [10.3390/ma14164428](https://doi.org/10.3390/ma14164428).
- [37] PN EN 14889-1:2007 Fibers for concrete – Part 1: Steel fibers – Definitions, specifications and conformity. Polish Committee for Standardization, Warsaw, 2007.
- [38] J.F. Olesen, "Fictitious crack propagation in fiber-reinforced concrete beams", *Journal of Engineering Mechanics*, vol. 127, no. 3, pp. 272–280, 2001, doi: [10.1061/\(ASCE\)0733-9399\(2001\)127:3\(272\)](https://doi.org/10.1061/(ASCE)0733-9399(2001)127:3(272)).
- [39] K.P. Juhász, "Modified fracture energy method for fiber reinforced concrete", presented at Fiber Concrete 2013, Prague, Czech Republic, Sept. 12–13, 2013.
- [40] A. Enfedaque, M.G. Alberti, J.C. Gálvez, and P. Cabanas, "Numerical simulation of the fracture behavior of high-performance fiber-reinforced concrete by using a cohesive crack-based inverse analysis", *Materials*, vol. 15, no. 1, art. no. 71, 2022, doi: [10.3390/ma15010071](https://doi.org/10.3390/ma15010071).
- [41] M. Pająk, M. Krystek, M. Zakrzewski, and J. Domski, "Laboratory investigation and numerical modelling of concrete reinforced with recycled steel fibers", *Materials*, vol. 14, no. 8, art. no. 1828, 2021, doi: [10.3390/ma14081828](https://doi.org/10.3390/ma14081828).
- [42] PN-EN 1917:2004 Studzienki włączowe i niewłączowe z betonu niezbrojonego, betonu zbrojonego włóknem stalowym i żelbetowe. Polish Committee for Standardization, Warsaw, 2004.
- [43] PN-EN 476:2012 Wymagania ogólne dotyczące elementów stosowanych w systemach kanalizacji deszczowej i sanitarnej. Polish Committee for Standardization, Warsaw, 2012.
- [44] FIB – International Federation for Structural Concrete, *Model Code 2010*. Lausanne, Switzerland, 2013.

Wytrzymałość na zginanie prefabrykowanych kręgów wykonanych z betonu zbrojonego włóknami syntetycznymi

Słowa kluczowe: fibrobeton, FRC, prefabrykowane kręgi, wytrzymałość resztkowa, włókna polimerowe

Streszczenie:

Od lat 90. XX wieku technologia betonu zbrojonego włóknami przeszła znaczący rozwój, który został zapoczątkowany przez publikację kompleksowego raportu komitetu ACI 544. Znormalizowano sposoby pomiarów kluczowych właściwości mechanicznych fibrobetonu w EN 14651 i ASTM C1609 oraz materiałowych w CEN/TS 19101. Powszechnie wiadomo, że dodatek włókien poprawia właściwości betonu, jednak skuteczność ich zależy od wielu czynników takich jak: rodzaj materiału (włókna metaliczne i niemetaliczne), kształt (włókna faliste i fibrylowane), wymiary (długość, średnica i smukłość), objętość w mieszance betonowej, a nawet konsystencji mieszanki. Celem przeprowadzonych badań doświadczalnych była ocena nośności betonu produkowanego w warunkach przemysłowych, modyfikowanego różnymi włóknami syntetycznymi o zróżnicowanym dawkowaniu. Docelowym kryterium wyboru włókien było spełnienie wymagań wytrzymałości resztkowej badanego elementu przy możliwie najmniejszym udziale wagowym zbrojenia rozproszonego. W trakcie prowadzonych badań oprócz wytrzymałości resztkowej PFRC, wyznaczono wytrzymałość na ściskanie, rozciąganie przy zginaniu oraz moduł sprężystości. Otrzymane wyniki oraz zależności siła-rozwarcie szczeliny, wykorzystano do walidacji modelu numerycznego normowej belki z nacięciem. Tak skalibrowany model materiałowy wykorzystano do budowy docelowego modelu MES i wstępnej oceny nośności fibrobetonowych kręgów prefabrykowanych w programie ATENA. Projekt "Regionalne Centrum Doskonałości w Inżynierii dla Jakości Życia i Rozwoju Technologii", finansowany z subwencji Ministra Nauki i Szkolnictwa Wyższego w ramach programu "Regionalna Inicjatywa Doskonałości" (projekt nr RID/SP/0032/2024/01).

Received: 2025-06-02, Revised: 2025-06-12